Manuscript 2

Quantifying Particle Hydrolysis and Observed Yield for a Full-Scale Biological Aerated Filter

Scott D. Phipps and Nancy G. Love
Charles E. Via Department of Civil and Environmental Engineering,
Virginia Polytechnic Institute and State University, Blacksburg, VA 24061-0246, USA

Abstract

Biomass observed yield values were calculated for a full-scale biological aerated filter (BAF). Three individual mass balances were conducted to quantify the consumption of soluble COD in the filter and the mass of influent particulate matter filtered from the waste stream. Retained particulate matter is a substrate source for the biomass; however, the particles must be hydrolyzed into metabolizable forms before being consumed by the biomass. A bench-scale BAF was designed and constructed to investigate the degree to which particle hydrolysis occurred in the full-scale system. Using two independent bench-scale BAF experiments, it was determined that 40.0 and 46.3% of influent particle mass as COD underwent hydrolysis. Additionally, fluorescein diacetate was used during one of the experiments as a model complex substrate to quantify the activity associated with hydrolytic enzymes in the bulk-liquid. Hydrolytic activity by cell-free extracellular enzymes in the bulk-liquid increased during the hydrolysis phase compared to the endogenous phase, which suggests that bulk-liquid hydrolysis may have contributed to the overall mechanistic degradation of particulate matter. Calculated biomass observed yields for the full-scale BAF ranged from 0.43 to 0.48 mg of biomass as COD generated per mg of substrate consumed as COD.

Keywords

Biological aerated filter, biomass yield, hydrolysis, extracellular enzymes

Introduction

Biological aerated filters (BAFs) are an emerging wastewater treatment technology designed for a wide range of municipal and industrial applications. BAFs use an inert media, either dense granular or floating, which supports biomass retention in the filter bed. Microorganisms utilize

carbonaceous material, ammonia, nutrients, and available oxygen for growth. A consortium of microorganisms are retained by the inert media either as surface-attached biofilms or in the interstitial pore spaces. Extracellular polymeric substances (EPS) are created by the biomass and structurally reinforce biomass attachment to the media. EPS is composed of monomers such as glucose, galactose, mannose, galacturonic acid, and glucuronic acid (Horan and Eccles, 1986; Characklis and Marshall, 1990). Various sized interstitial voids, channels, and globular cell masses are dispersed throughout the biofilm and liquid-biofilm interface. These structural features increase the liquid-biofilm interface to maximize exposed surface area and facilitate mass transfer of substrate and nutrients into the biofilm (de Beer, et al., 1993; Lewandowski, et al., 1994, Stoodley, et al., 1994).

BAFs offer an alternative to typical biological treatment processes; however, knowledge of the process is often limited, especially in the US market. Since the late 1980s, BAF systems have been extensively studied and applied in Europe (Pujol et al., 1994; Carrand, et al., 1990; Sagberg, et al., 1992; Amar et al., 1986; Richard, et al., 1987). Through various studies, process improvements were made for filter media selection, backwash protocols, and hydraulic load effects (Pujol, 2000; Song, et al., 1986). European implementation and reported BAF performance successes increased interest for this technology as a possible wastewater treatment alternative in the United States.

Biomass yield is an important design parameter for biological treatment systems. The biomass yield parameter is defined as the mass of biomass produced per mass of substrate consumed, usually expressed in COD units. Biomass yield values are important in determining the wastage rate from a biological treatment system. Essentially, a biological treatment system must waste the mass of biomass generated daily; otherwise, an accumulation of biomass will occur. Biomass yields are site and waste stream specific; however, 70 years of experience with activated sludge systems has resulted in designers having a reasonable level of confidence in estimating biomass yields for design. The BAF treatment system does not have the same level of experience, and few biomass yield estimations are publicly available for use during design. Accurate biomass yield estimates are required before BAF systems can be designed, operated, and managed properly.

Biomass yield estimates aid in the design of aerobic biological treatment systems in two ways. First, yield is an important input parameter for determining required oxygen. An electron acceptor is required for the oxidation of wastewater constituents and for supporting endogenous metabolism by the biomass. Oxygen demands in aerobic treatment systems include the oxidation of applied biodegradable substrate and biodegradable substrate available from particle hydrolysis. Particle hydrolysis increases the oxygen demand in treatment systems by increasing the biodegradable soluble COD susceptible to biological oxidation. Therefore, the quantification of particle hydrolysis and the associated yield values are important when determining the oxygen requirements and designing aeration systems for biological treatment systems. Aeration is a significant cost associated with biological wastewater treatment. If biomass yield estimates are known, the aeration system can be effectively designed to degrade influent wastewater while minimizing costs. Air process blowers and aeration equipment need to be properly design for both treatment performance and cost effectiveness. Second, biomass yield estimates also aid in the design of solids handling facilities. Biomass must be wasted at or near the same rate as it is generated. If biomass yield estimates are available, then required capacities for handling and storing biosoilds from the treatment process can be designed. Clearly, knowledge of biomass yield will benefit in the design of aeration systems and solids handling facilities at biological wastewater treatment facilities.

Biomass yields are estimated by comparing the amount of biomass formed relative to the amount of pollutant eliminated from the waste stream. Substrate consumption is partitioned into two separate biological functions. A fraction of the energy obtained from substrate is used for cell growth and maintenance, and the remaining substrate energy is used to form new cells. The formation of new cells represents the biomass yield. Biomass yields are classified into two categories. First, the true growth yield is defined as the mass of biomass generated per substrate consumed, ignoring biomass decay by cell lysis and death. The observed biomass yield incorporates biomass decay into the yield value. Various studies and investigations have estimated biomass yields from biological systems. Biomass yields have been intensively studied for denitrification systems (Ong, et al., 2000; Koch, et al., 1997; Barlindhaug, et al., 1996; Aesoy, et al., 1994), nitrification systems (Green et al., 2001), anaerobic systems (Arcangeli, et al., 1997; Pavlostathis, et al., 1991), and industrial wastewater treatment systems degrading

specific compounds (Antizar-Ladislao, et al., 2000; Karamanev, D., 1998, Arcangeli, et al., 1994). Yield estimates were simplified in these studies either because the wastewater was primarily soluble and its consumption could be easily measured, or because catabolism by-products, such as methane from anaerobic systems, could be easily measured. A major challenge in determining biomass yield for domestic wastewater treatment is quantifying the fraction of influent particulate matter that undergoes hydrolysis and is subsequently consumed as a substrate source.

Particle hydrolysis is an important biological function of biological treatment systems when eliminating large molecular weight substrates from the waste stream. Domestic wastewater's composition is site-specific and individual waste streams vary, but the typical composition of wastewater contains 40-60% proteins, 25-50% carbohydrates, and 10% lipids (Metacalf and Eddy, 1991). A range of particle sizes are found in municipal wastewater, and larger particles of proteins, called polypeptides, and carbohydrates, called polysaccharides, are often in high concentrations (Levine et al, 1985). Unlike soluble materials, particles cannot pass through cellular membranes due to their large molecular size. Hydrolysis of these larger particles is required before the biomass can completely oxidize and remove them from the waste stream. Particulate matter must be hydrolyzed into metabolizable monomers before consumption and utilization as an available substrate.

Mass transfer of particles to the biomass is often the limiting step in the hydrolysis of particles into smaller monomers. Mass transfer coefficients for particles are small relative to soluble substrates (Logan, et al., 1987a). Three mechanisms control particle mass transfer in biofilm reactors. The first controlling mechanism is molecular diffusion. Large particles must diffuse through the bulk liquid to the liquid-biofilm boundary layer, which is a boundary between the bulk liquid and exterior of the biofilm. Particle size and surface charge dictate the diffusion through the liquid-biofilm boundary layer. Liquid-biofilm boundary layer retardation, such as steric hindrances and repulsive electrostatic interactions, decrease particle mass transfer coefficients through the liquid-biofilm boundary (Bouwer, 1987). Once through the liquid-biofilm layer, particles must migrate through the biofilm voids and channels to find attachment sites. Possible attachment sites are extracellular polymeric substances (EPS), cell walls, or

cytoplasm membranes (Fleming, 1995). The rate of particle diffusion increases with decreasing particle size once inside the liquid-biofilm boundary layer. Larger particles will only penetrate to shallow biofilm depths, whereas smaller particles can infiltrate into deeper regions of the biofilm. Particle mass transfer by diffusion requires migration through the bulk liquid to the liquid-biofilm layer, overcoming retardation effects, and attaching to the biofilm layer.

The second particle mass transfer mechanism is particle sedimentation (Bouwer, 1987). Particle sedimentation is due to gravity and physical properties of individual particles, such as size and density. The settling velocity calculated from Stoke's Law can describe particle sedimentation in biofilm systems (Bouwer, 1987). Particle sedimentation is often limited in up-flow reactors due to the countercurrent movement of the liquid. Sedimentation mass transfer is directly dependent upon the fluid velocity in up-flow reactors. If the up-flow fluid velocity exceeds the particle's settling velocity, the particle will be washed out of the system. Larger particles with faster settling velocities can overcome up-flow fluid velocities and settle in biofilms located on the downstream side of the media. Additionally, biofilm surface roughness will increase sedimentation of particles (Siegrist and Gujer, 1985). Biofilm voids and channels create pools of slow moving liquid, which will facilitate sedimentation. These pockets of "stagnant" liquid will minimize fluid velocities and decrease the countercurrent fluid action present in up-flow reactors. Additionally, the heterogeneous biofilm voids, channels, and cell masses increase the available surface area where particle deposition and attachment can occur. Particle sedimentation is an important mass transfer mechanism for attachment and enmeshment of particles in biofilm systems.

The final mass transfer mechanism of particles is due to fluid shear effects (Bouwer, 1987). Fluid velocity in biofilm reactors can control particle attachment in three separate ways. First, increased fluid velocities will decrease the thickness of the liquid-biofilm boundary layer. A liquid-biofilm boundary layer decrease will facilitate the passage of particles through the layer and promote increased particle attachment. The second method increases particle attachment by forcing particles to collide with the biofilm in the process known as interception (Bouwer, 1987). High fluid velocities will increase the collisions of particles to biofilms, which increase the opportunities for attachment. The third mass transfer mechanism caused by fluid velocity

detaches particles due to high shearing effects. Increased fluid velocities shear attached particles and biofilm mass from the inert media. However, the detachment of particles and biomass is decreased due to the heterogeneous biofilm exterior and surface roughness as stated previously. Fluid shear increases particle attachment by decreasing the thickness of the liquid-boundary layer and increasing particle interception, but also dislodges attached particles due to high shear stresses.

After mass transfer limitations have been overcome, hydrolysis is required to transport the hydrolyzed monomers into biofilms and individual cells of fixed-film system (Logan et al., 1987a,b; Confer and Logan, 1991). Currently, two hypotheses have been proposed to describe the mechanistic degradation and hydrolysis of particles. Both hydrolysis hypotheses require membrane-bound extracellular enzymes to hydrolyze particles attached to the biofilm. However, one hypothesis suggests cell-free extracellular enzymes (CFEE) hydrolyze large particles in the bulk-liquid as an initial step. This bulk-liquid hydrolysis by CFEEs reduces particle size and promotes particle attachment to biofilms. After biofilm attachment, membrane-bound extracellular enzymes (MBEE) perform additional particle hydrolysis and subsequent uptake and consumption by the cells. The second hypothesis suggests only MBEE hydrolyze particles before transport into cells.

Larsen and Harremoës (1994) proposed a hydrolysis hypothesis, which combines both CFEE and MBEE hydrolysis reactions. A model was formulated to analyze the mechanism of colloidal organic matter degradation in biofilm reactors (Larsen and Harremoës, 1994). The hypothesis and model involve the production of CFEE by microorganisms located in the biofilm and subsequent release into the bulk liquid. The CFEE released into the bulk liquid hydrolyze particles and create intermediate-sized monomers in the bulk liquid. These hydrolyzed monomers molecularly diffuse through the liquid-biofilm layer more readily, and biofilm attachment is promoted. The second phase of the hypothesis requires MBEE to further hydrolyze the intermediate-sized monomers before passage through cellular membranes. In their investigations, cell-free, i.e. bulk-liquid, hydrolysis dominated the biofilm activity in a bench-scale biofilm reactor (Larsen and Harremoës, 1994). Other research indicates cell-free

hydrolysis dominates in natural environments as well (Hoppe, 1983; Somville and Billen, 1983; Chróst, 1989).

The second hydrolysis hypothesis was proposed by Confer and Logan (1997a), which states bulk liquid hydrolysis is negligible, and MBEE supports the only means of particle hydrolysis. Overcoming limitations of molecular diffusion and surface attachment are the first steps in the hypothesis. After biofilm attachment, MBEE cleave molecular bonds to reduce particle size. Intermediate sized oligomers of particles remain attached to the biofilm or are released from the biofilm into the bulk-liquid. Particle hydrolysis requires several specific enzymes for complete "solublization" into the biofilm, and the release of the intermediate sized oligomers is induced because available MBEE cannot cleave any additional bonds. Therefore, hydrolysis stops until the necessary enzymes are available. The released intermediate sized oligomers will diffuse away from the cell membrane into the bulk liquid. The intermediate sized oligomers molecularly diffuse back across the liquid-biofilm layer at another location and reattach to the biofilm. This mechanism of detachment and reattachment continues until the particle is completely hydrolyzed and consumed by cells. This hypothesis is supported by research performed by Confer and Logan (1997a and 1997b) when studying protein and polysaccharide particle hydrolysis.

Protein material found in wastewater is predominantly in the form of polypeptides (Confer and Logan, 1997a; Confer, et al., 1995), which require hydrolysis before cellular uptake. Polypeptide hydrolysis into amino acids has been found to be predominantly membrane-bound (Boczar, et al., 1992; Hollibaugh and Azam, 1983). Confer and Logan (1997a) investigated bovine serum albumin (BSA) as a model macromolecule of protein in suspended and biofilm cultures. Intermediate sized BSA monomers did not accumulate in the bulk liquid of a rotating biofilm reactor. The lack of intermediate sized BSA monomer accumulation indicates that BSA was hydrolyzed by MBEE rather than in the bulk liquid (Confer and Logan, 1997a; Holibaugh and Azam, 1983). Another study showed no accumulation of intermediate sized proteins in an activated sludge system treating a meat packing wastewater (McLoughlin and Crombie-Quilty, 1983). These studies seem to support Confer and Logan's hypothesis of MBEE providing the only hydrolytic function; however, Larsen and Harremoës's hypothesis of cell-free hydrolysis is not disproven. Intermediate sized protein molecules did not accumulate in the bulk liquid, but

molecular diffusion may have been enhanced by an initial bulk liquid hydrolysis step, as proposed by Larsen and Harremoës. The initial bulk liquid hydrolysis may have promoted the attachment of intermediate sized protein to the biofilm, which decreases the concentration of intermediate sized proteins available for measurement and accumulation in the bulk liquid. Therefore, both hypotheses need further study before any conclusions can be made.

Additional investigators analyzed polysaccharide hydrolysis as well. Carbohydrates in wastewater exist as simple sugars, dissolved macromolecules, EPS, and large particulate polysaccharides (Pavoni, et al., 1972; Tago and Aida, 1977). Small carbohydrate molecules diffuse through the liquid-biofilm boundary layer readily and are immediately available as microbial substrate. However, polysaccharides larger than 1000 atomic mass units (amu) do not pass through cellular membranes and require hydrolysis before becoming available as substrate (Confer and Logan, 1997b). Similar to protein hydrolysis, polysaccharides require numerous hydrolytic enzymes before assimilation into cells. The hydrolytic mechanism of polysaccharides has been intensively studied. Research investigations have analyzed the molecular size distributions of dextran (a polymer of glucose) during hydrolysis experiments in batch and continuous cultures (Haldane and Logan, 1994; Confer and Logan, 1997b). Oligomeric polysaccharides, hydrolyzed polysaccharides residuals too large for consumption, did accumulate in the bulk liquid during these investigations, and the authors suggested that multiple enzymes are required for complete hydrolysis (Haldane and Logan, 1994) or bulk liquid hydrolysis by CFEE to occur. Bulk liquid hydrolysis by CFEE may have contributed to the accumulation of oligomeric polysaccharides in the bulk liquid, which supports Larsen and Harremoës's hypothesis. An additional study by Confer and Logan (1997b) with dextran revealed oligomeric polysaccharides were released into the bulk liquid by cells, which supports their hypothesis. Again, more research and investigations into particle hydrolysis are necessary before any conclusion can be made.

Biofilm and enzyme activities have been investigated quite thoroughly in the last twenty years. Lazarova and Manem (1995) give an extensive review of biofilm activity descriptors by enzyme analyses and investigations of microbial metabolism products. ATP determination, measurement of electron transport system activity (ETS), INT-dehydrogenase activity (DHA), and RNA/DNA

measurement by spectrophotometry and radioisotope labeling are all methods of quantifying biofilm activity (Larzarova and Manem, 1995). Additionally, fluorescein diacetate (FDA) hydrolysis has been used as an indicator of hydrolytic enzyme activity in activated sludges (Fontvieille, et al., 1992) and soils (Schnurer and Rosswall, 1982). Also, FDA hydrolysis has also been used to quantify microbial biomass on coniferous needles (Swisher and Carrol, 1980). FDA hydrolysis requires the removal of ester-linkages on the FDA molecule to form fluorescein, which fluoresces a brilliant yellow-green color. FDA is hydrolyzed by extracellular esterase enzymes that are common in bacteria (De Rosa, et al., 1995); therefore, FDA hydrolysis is a general indicator of hydrolytic enzyme activity.

This study investigated and determined the observed biomass yield for a full-scale BIOFOR® biological aerated filter. Mass balances were performed on the full-scale system to measure soluble substrate consumption and particulate enmeshment in the filter. A bench-scale system was design to mimic the full-scale system for particulate hydrolysis experiments. The particle hydrolysis values calculated from the bench-scale reactor were used to estimate particle hydrolysis on the full-scale system. The bench-scale system allowed the completion of the full-scale mass balance and the calculation of the observed biomass yield. Additionally, FDA hydrolysis was used to analyze CFEE enzyme activity in effluent samples from the bench-scale biofilm reactor. The measurement of cell-free extracellular enzyme activity was used to further support one of the proposed macromolecule degradation hypotheses.

Material and Methods

Full-Scale BAF System Description

The full-scale BIOFOR® used during this study has a 10 MGD average design flow (14 MGD maximum flow) and is operated as a side stream treatment process to an existing activated sludge system. The BAF consists of two-stages. Six separate first-stage cells (C-unit) remove carbonaceous material from screened primary effluent. Each individual cell has a surface area of 96 m^2 (1,034 ft^2) and a media depth of 3.9 m (12.8 ft). Influent wastewater (primary effluent) to the BAF is pretreated with two parallel arc screens. After initial arc screening, wastewater flows into six separate, meshed, head boxes for additional solids screening. The screened wastewater is applied from the cell's plenum to achieve upflow treatment. A retention weir prevents media washout, and treated wastewater flows into a discharge channel. The second-stage (N-unit)

consists of six separate cells designed for nitrification. All full-scale biomass yield investigations were conducted on the first-stage cells, the C-unit, for the removal of carbonaceous material.

Maximum filter run time or pressure differential dictates when filter backwashing occurs. The C-unit cells are allowed a maximum run time of 24 hours between backwashes, and the maximum pressure differential allowed is 40 inches of water. Typically, maximum pressure differential dictates filter run times. The backwash includes several high velocity air/water stages, phases for media settling, and final media rinses. Individual process blowers supply air for scouring, while treated BAF wastewater is used for water scour. Each cell is isolated during backwashes, and a separate holding tank collects backwash waste. Backwash waste is blended with the facility's raw wastewater so that backwashed solids can be removed through primary sedimentation.

Mass Balance Sample Collection

Influent and effluent samples

Influent and effluent samplers were constructed to collect samples from a single C-unit cell. The influent sampler was located at the head box to the cell, while the effluent sampler collected liquid flowing only from the investigated C-unit cell. One-quarter inch tubing was used with the sampler and was placed a minimum of 6" below the water surface. The sample tubing was covered with foam insulation to prevent freezing. A constant 10 mL/min sample was collected to further prevent freezing in the sampling tubes. The influent and effluent samplers consisted of a pump controller, peristaltic pump, and a five-gallon plastic collection vessel. The entire sampling system was placed inside a 30-gallon trash can and was insulated with material to prevent sample freezing. The samplers were started at the completion of a backwash sequence. Sampling continued for the entire cell run time. Sampling was stopped immediately before the start of the next backwashing sequence. The temperature of applied influent wastewater varied between 14.6 °C and 21.3 °C on three different days when mass balances were performed. Samples were stored in accordance with Standard Methods (APHA, 1995). Total COD, soluble COD, and TSS/VSS analyses were performed in triplicate on both influent and effluent composite samples. COD values associated with particulate material (>1.5 µm) were calculated from the difference between measured total and soluble COD.

Backwash samples

Backwash samples were collected during the backwash sequence for an individual filter cell. Grab samples (750 mL) were collected each minute of the entire backwash cycle (35 minutes) using a long steel pole containing a collection cup. Samples were collected downstream of the media retention weir. The 750 mL grab sample was poured into a 500 mL container and stored in a cooler during transport. A backwash composite sample was formed by pooling 25 mL of well-mixed volume from each of the 35 backwash samples, and the backwash composite sample was stored according to Standard Methods (APHA, 1995). COD, soluble COD, and TSS/VSS analyses were performed in triplicate on the backwash composite sample.

Bench-Scale BAF Reactor

The bench-scale reactor was constructed from a plastic 250-mL graduated cylinder. A one-quarter inch (1/4) hole was drilled through the base of the graduated cylinder, and an influent port was inserted into the drilled hole. This design allowed influent to be pumped through the column in an upflow fashion. Eight, one-eighth (1/8) inch OD ports were installed along the entire column one inch apart on center. The ports had one thirty-second (1/32) holes drilled in a crisscrossing pattern. The ports were sealed with two-inch long bolts, which stabilized the ports. The ports were sealed with epoxy to prevent leakage. In the original column design, the ports were to be used as input points for injecting particles, which would create excellent particle distribution. However, portal use during operation was ineffective because of column resealing and loss of applied particulate material. Therefore, the portals were not used for particle addition during the experiments. Figures 1 and 2 show detailed schematics of the bench-scale reactor and experimental system.

The media, called Biolite, is expanded clay with a high specific surface area (400 – 500 ft^2/ft^3) and low density. Approximately 4 gallons of media was collected from a first-stage C unit cell in the full-scale BAF system during a plant shutdown. A portion of the media was washed vigorously five times with distilled water to remove any particulate matter entrained in the media pores. After rinsing, the media was stored at room temperature in a five gallon bucket. Media

was placed into the bench-scale reactor with a small spoon, and the column was shaken to minimize the interstitial pore space by compacting the media. The media depth was eight inches

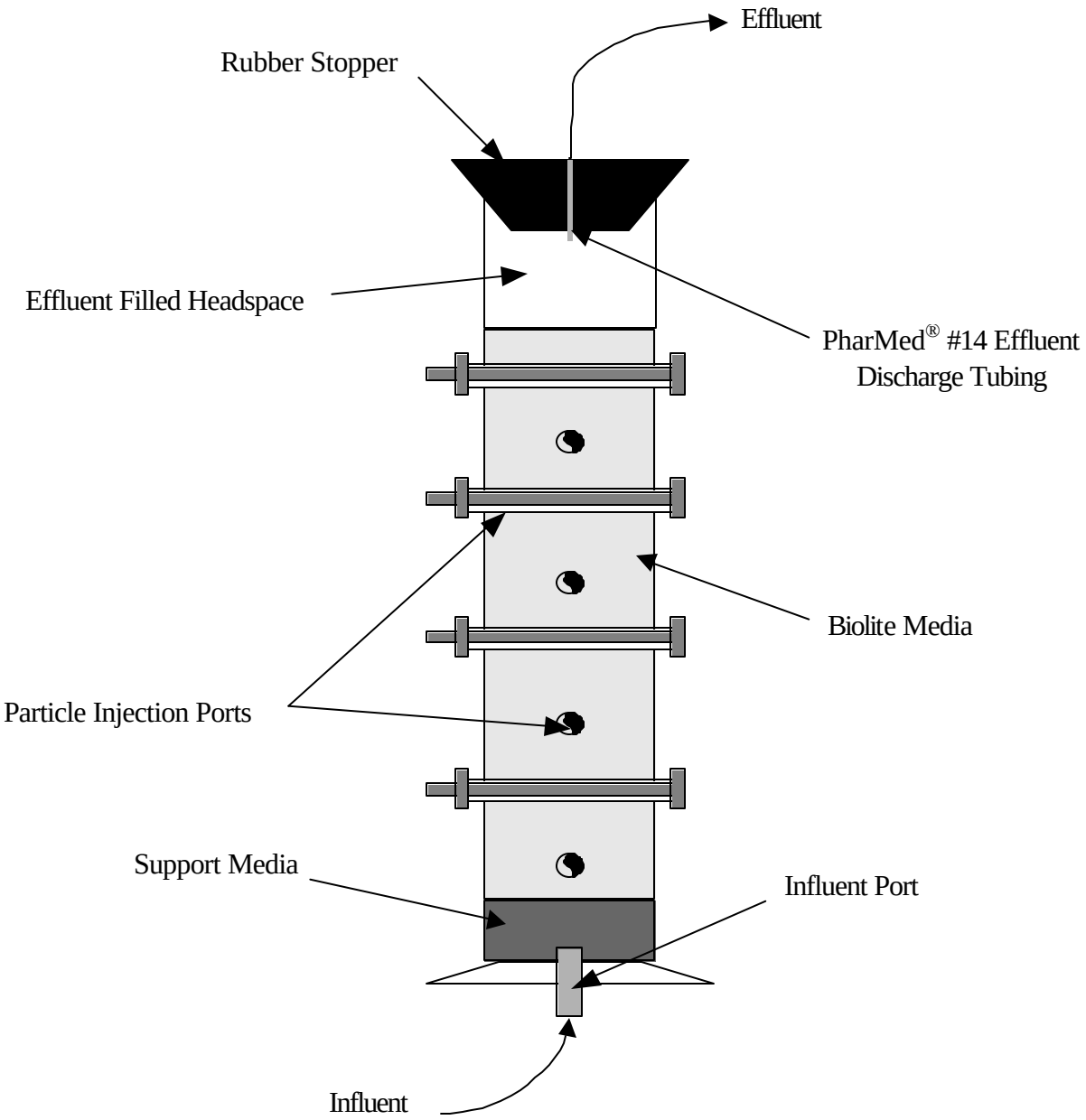

Figure 1: Schematic of Bench-Scale Reactor Utilized During Particle Hydrolysis Experiments

and was supported by one-inch depth of 8 mm plastic beads. A rubber stopper was placed in the top of the column to ensure zero headspace. The rubber stopper allowed the system to be

pressurized so that the oxygen present in the column had to come from air dissolved in the liquid pumped into the column. Effluent discharged through a sealed one-sixteenth (1/16) inch hole bored in the stopper and fixed with a three and one-half (3-1/2) inch long PharMed® #14 effluent discharge tube. The hydraulic residence time (HRT) was determined to be 65 minutes using a tracer test (see Appendix A). This is comparable to the HRT in the full-scale system, which has a calculated contact time (pore volume only) of 1.1 hours.

Dissolved Oxygen (DO) measurement

Dissolved oxygen was measured by two Model 97-08 oxygen electrodes (Orion, Beverly, MA). The electrodes were connected to an Accumet® Research AR 25 Dual Channel pH/Ion meter (Fisher Scientific). The electrodes measured partial pressure of oxygen rather than dissolved oxygen concentration; therefore, millivolt readings were calibrated to known DO values. The electrodes were modified by removing the stirring mechanism and adding a rubber stopper onto the electron probe. The rubber stopper was bored and slipped onto the electrode to supply an air-tight seal on two modified 300-mL BOD bottles. The BOD bottles had two glass ports installed for influent and effluent flow. The inlet to the bottle was located near the base, whereas the outlet was near the bottle's neck. Two Thermolyne Cimarec 2 stir plates were used with two, one and one-half (1-1/2) inch stir bars placed in the BOD bottles to ensure adequate mixing.

Data Acquisition

Data acquisition consisted of a Dell Latitude XPi laptop computer, Accumet® Research AR 25 Dual Channel pH/Ion meter (Fisher Scientific), and two model 97-08 oxygen electrodes (Orion, Beverly, MA). A LabView (version 6.0, National Instruments, Austin, TX) program was written to record readings from both oxygen electrodes every 3 seconds. Final output data were manipulated so that every 20 readings were averaged to yield a data point for every minute of reactor operation.

Bench-Scale Reactor Sample Collection

Bench-scale reactor composite samples were collected in one-liter glass beakers and stored at 4° C in a refrigerator. After collection, composite samples were removed from the refrigerator and stirred on a Thermolyne Cimarec 2 stir plate with a one and one-half (1-1/2) inch stir bar.

Samples were transferred by 30 cc disposable syringes into 25 mL scintillation vials. Samples were either deposited directly into the vials as a total (soluble plus insoluble) fraction, or were filtered through a 1.5 µm pore size Whatman 934-AH glass microfiber filter (rinsed with distilled water and ignited at 550° C for a minimum of 45 minutes before use). Samples filtered through the 934-AH glass microfiber filter were classified as soluble.

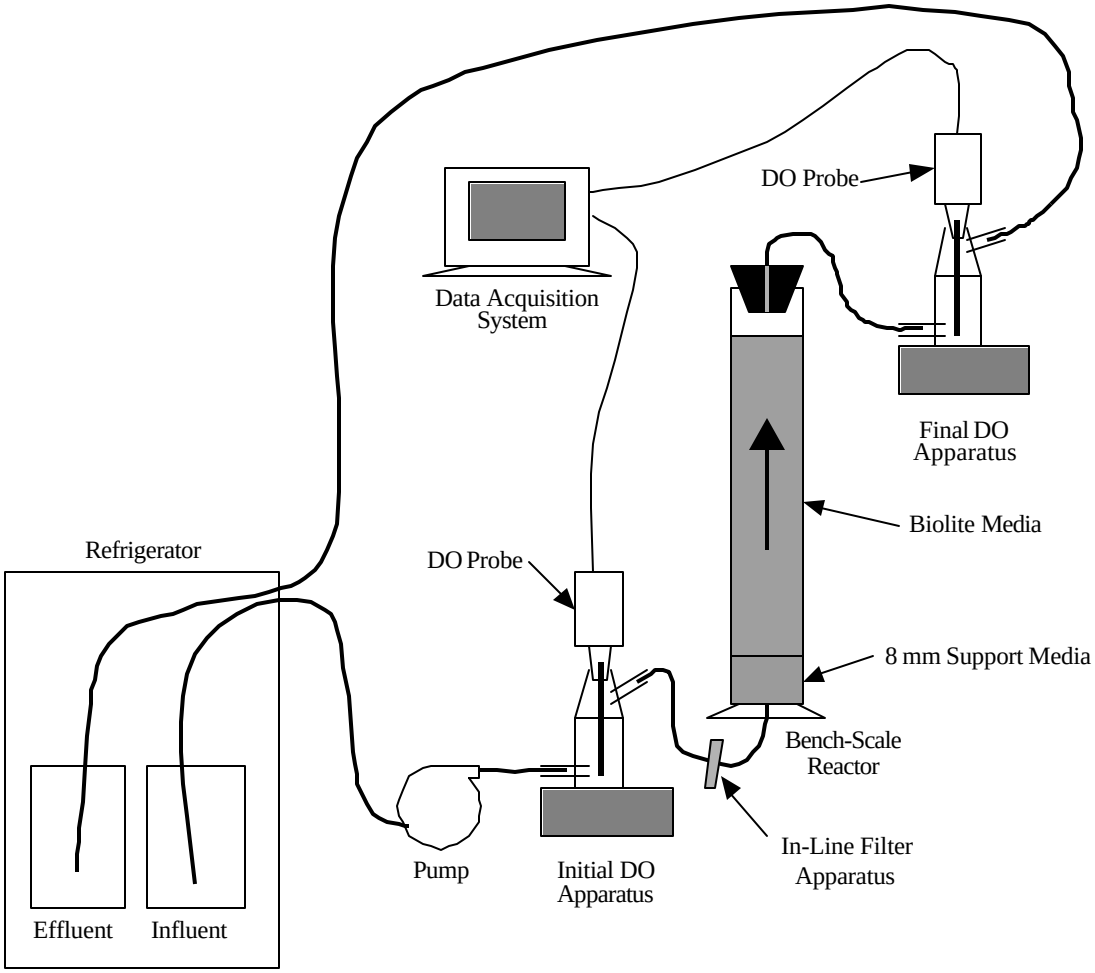

Figure 2: Schematic of Bench-Scale System Utilized During Particle Hydrolysis Experiments

Sample collection and analyses for bench-scale hydrolysis experiments

COD, soluble COD, nitrate/nitrite, and enzyme samples were collected on a scheduled sampling regime (see Table 1) during endogenous and hydrolysis phases (described below). COD and soluble COD samples were acidified with concentrated sulfuric acid and stored at 4° C until

analyzed according to method 5220-C in Standard Methods (APHA, 1995). Nitrate (NO_3^-) and nitrite (NO_2^-) samples were frozen until analyzed using ion chromatography (DIONEX model DX-120, Sunnyvale, California) with automated data acquisition, conductivity detection, an AS40 automated sampler, and Chromeleon analysis software. All samples were analyzed according to method 4110 B in Standard Methods (APHA, 1995).

Table 1: Sampling Regime for Endogenous and Hydrolysis Phase of Bench-Scale Reactor Operation

Sample Number	Sample Collection Time (Hours)
1	0.5
2	1.0
3	1.5
4	2.0
5	3.0
6	4.0
7	6.0
8	9.0
9	13.0
10	18.0
11	24.0

Extracellular enzyme assays were analyzed on samples immediately after collection using a modified fluorescein diacetate (FDA) procedure outlined in Fontvieille, et al. (1992). Ten mL sterile test tubes were autoclaved and used for the FDA procedure. Enzyme assays were performed on total (unfiltered) samples as well as two types of soluble samples (1.5 µm filtered, per description above, and 0.45 µm Gelman Laboratory Supor®-450 filtered). FDA blanks and duplicate test tubes were analyzed for all three samples collected. An effluent sample of 4 mL was pipetted into 2 mL of 0.1 M phosphate buffer (pH = 7.47) in a 10 mL sterile test tube. 0.1 mL of FDA (Sigma Chemical, St. Louis, MO) reagent (dissolved in HPLC grade acetone to a final concentration of 4.83 mM) was pipetted into each test tube . FDA was introduced into the test tube just beneath the liquid-air interface to minimize precipitation of FDA. The test tube was vortexed for 10 sec and was incubated for 6 hours at 20° C. Following the 6 hour incubation time, samples were poured from the incubation test tubes into 15 mL Corning centrifuge tubes. Samples were centrifuge for 5 minutes in a Centrific™ Centrifuge (Fisher Scientific) at a speed

of 8.5 (approximately 4,200xg). After centrifugation, absorbance was measured on a Beckman DU® 640 spectrophotometer (Palo Alto, CA) at 490 nm wavelength using the sipper mechanism. Each assay was analyzed in triplicate with a Nanopure flush between samples.

Growth on Primary effluent

Primary effluent was used as influent feed during the growth and re-growth phases (described below). Primary effluent samples were collected from the full-scale BAF facility using a five gallon bucket. Samples were collected from the primary clarifier surface. The samples were transported to the laboratory, where the samples were stored at 4° C until use. Primary effluent samples were allowed to settle for a minimum of 4 hours to minimize filtering required. Settled primary effluent was bailed from the five-gallon collection vessel with one liter plastic containers to minimize disturbance of settled particulate matter. The bailed primary effluent was filtered through Whatman 52 Filter papers (hardened circles, 110 mm diameter, 7 µm pore size) to eliminate large particles and debris. Filtrate was filtered a second time through Whatman 934-AH glass microfiber filters (circles, 55 mm diameter, 1.5 µm pore size). Filtered primary effluent was purged with pure oxygen to achieve an initial concentration between 10 and 14 mg/L before pumping it as influent into the bench-scale reactor.

Particle solution

Primary effluent was collected from the full-scale BAF and transported to the laboratory. Samples were collected in a similar fashion to the primary effluent used during the growth and re-growth phase. Primary effluent was allowed to settle for a minimum of 8 hours. Supernatant from the storage vessels was removed with one-liter plastic containers to reduce the volume for centrifugation. The settled particles were placed in 500 mL centrifuge tubes and centrifuged at 11,300xg in a Beckman J2-HS centrifuge (Palo Alto, CA). After centrifugation, the supernatant was discharged and the residual pellets were retained. Pellets were resuspended in a mineral salt solution (see Table 2). The particle solution was mixed on Thermolyne Cimarec 2 stir plate with a one and one-half (1-1/2) inch stir bar for 6 hours to insure adequate resuspension of particles. COD and soluble COD samples were collected, acidified, and stored for later analysis.

Mineral salts

A mineral salt solution (18 L) was prepared with the composition given in Table 2, and was stored in a 20 L glass reservoir. The mineral salt solution was stored at 4° C to minimize contamination.

Table 2: Mineral Salt Solution Used during Endogenous Respiration and Hydrolysis Phases

Constituent	Concentration (mg/L)
Potassium	3.1
Calcium	4.6
Magnesium	4.3
Sulfur	3.3
Sodium	2.1
Chloride	1.9
Iron	0.6
Zinc	0.05
Manganese	0.1
Copper	0.007
Molybdenum	0.001
Cobalt	0.1

Bench-Scale Reactor System Operation

The bench-scale reactor was operated with several phases at room temperature (approximately 20 °C). The pump and data acquisition system were turned on at the start of a phase and stopped at the phase's completion. After phase completion, the next phase's feed, whether filtered primary effluent or mineral salts, was purged with pure oxygen to a DO concentration between 10 and 14 mg/L. The entire system was refilled with the purged feed and the pump and data acquisition system were restarted.

A hydrolysis experiment consisted of four separate and distinct phases: growth, endogenous respiration, re-growth, and hydrolysis. The growth and re-growth phases of the experiment used full-scale BAF soluble (<1.5 µm) influent wastewater as feed, which established biomass growth in the bench-scale reactor. By using a soluble influent, it was possible to ensure that all particles contained in the filter were biomass-associated. The growth phase lasted approximately 10 hours in the first experiment and 14 hours in the second experiment. The re-growth phase was used to re-establish the biomass of the endogenous phase for a physiological comparison between the

endogenous and hydrolysis phases. The first experiment had a re-growth phase lasting approximately 12 hours, and the second experiment re-growth phase operated approximately 6 hours. The endogenous respiration phase lasted 24 hours for both experiments utilizing a mineral salt feed (see Table 2). The experimental run time of 24 hours was used because the set filter run times at the full-scale system last 24 hours. The data acquisition system was used to collect initial and final DO concentrations throughout both phases, and COD and soluble COD composite samples were collected during the endogenous respiration phase on a pre-arranged sampling regime shown in Table 1. The different phases and corresponding influent feeds are shown in Figure 3.

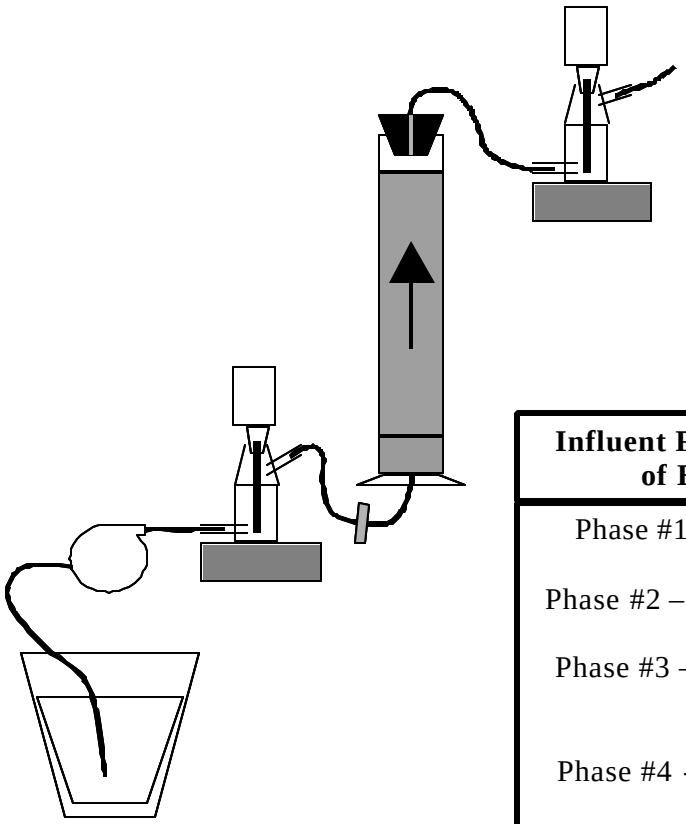

Influent Feed Used During Different Phases of Each Hydrolysis Experiment	
Phase #1 – Growth	Filtered 1° Effluent
Phase #2 – Endogenous	Mineral Salts
Phase #3 – Re-growth	Filtered 1° Effluent
Phase #4 - Hydrolysis	Mineral Salts (with a spike input of particles)

Figure 3: Schematic of Bench-Scale Reactor and Applied Feeds During Different Phases

A procedure was established to introduce a known mass of particles into the column during the hydrolysis phase. The system was filled with mineral salts to the influent port at the reactor base and was clamped by forceps as shown in Figure 4. The bench-scale reactor was then filled through the reactor's base with a known mass of particles suspended in mineral salts. The

clamped influent tube was then installed on the influent port, and the remaining system volume was completely filled with mineral salt solution as shown in Figure 4. The particle solution was introduced into the column after the influent DO probe (see Figure 4); therefore, the particle solution was also purged with pure oxygen to a concentration within 0.1 mg/L of the mineral salt solution. A fish pump was used to strip out the additional oxygen if the particle solution become over-saturated. Oxygen addition and required oxygen stripping was repeated until the dissolved oxygen concentration of the particle solution and mineral salt solution were within $\pm$ 0.1 mg/L of each other.

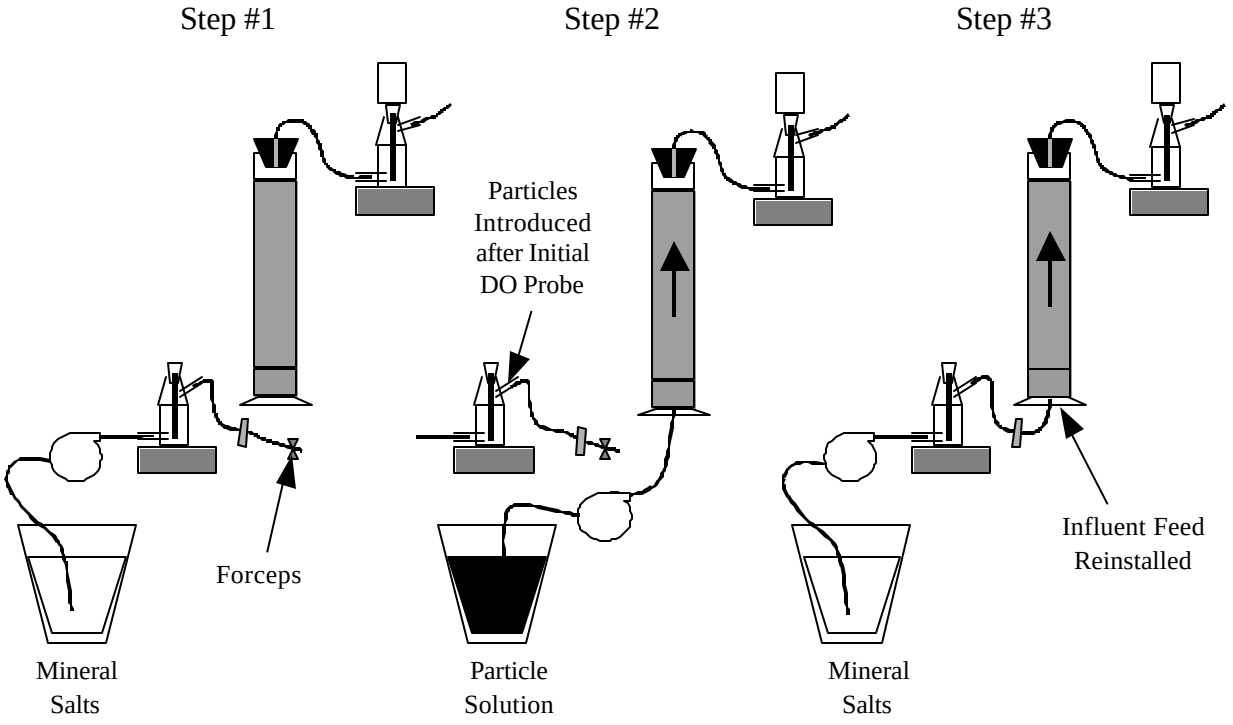

Method of Particle Introduction into Bench-Scale Reactor for a Spike-Input

Step #1: The influent tube is filled with mineral salt solution to the base of the reactor and clamped with forceps

Step #2: Particle solution is added to the column to the top of the reactor

Step #3: Influent tube is re-installed on the influent port located at the base of the reactor and mineral salt is added until the entire bench-scale reactor is filled with fluid

Figure 4: Schematic of Particle Introduction Method into the Column Prior to Both Hydrolysis Phases

Results and discussion

Full-Scale BAF Mass Balances

Three separate mass balances were performed on an isolated first-stage (C-unit) BIOFOR® BAF cell. TSS, VSS, COD, soluble COD, and particulate COD values from the mass balances are summarized in Table 3.

The BAF treatment system was successful at removing solid materials from the applied influent wastewater. TSS removal percentages ranged from 89 to 96% and VSS removal varied from 87 to 96% during the performed experiments. Applied influent wastewater must travel through a tortuous path of media pores within the filter bed, and the media retains the solid material that is unable to successfully maneuver through the pore spaces. Additionally, the BIOFOR® media is very angular and not uniform, which also increases the filtering of solid material. The depth of media (3.9 m, 12.8 ft) is another feature, which enhances the filtering of solid material. The media and deep media bed do not allow an easy travel path for applied wastewater; therefore, the filter bed's solids retention ability is exceptional. Clearly, a high percentage of applied solids were retained within the filter.

Table 3: Mass Balance Data from the Full-Scale Biological Aerated Filter

Parameter	Location	Experiment #1 (kg)	Experiment #2 (kg)	Experiment #3 (kg)
TSS	Influent	552 ± 12.0	546 ± 17.1	476 ± 41.1
	Effluent	61 ± 4.3	52 ± 11.8	18 ± 3.9
	%Removal	89%	90%	96%
	Backwash	819 ± 18.7	700 ± 20.3	767 ± 39.6
VSS	Influent	466 ± 2.9	424 ± 2.0	371± 3.2
	Effluent	59 ± 4.1	42 ± 6.5	17 ± 4.5
	% Removal	87%	90%	95%
	Backwash	650 ± 9.9	464 ± 70.1	602 ± 48.5
COD	Influent	2193 ± 83.6	1829 ± 50.6	1908 ± 29.6
	Effluent	551 ± 40.6	520 ± 5.9	442 ± 0
	% Removal	75%	72%	77%
	Backwash	1056 ± 90.8	844 ± 13.8	974 ± 22.7
sCOD	Influent	1173 ± 8.2	909 ± 38.8	878 ± 19.4
	Effluent	486 ± 20.0	427 ± 33.0	386 ± 11.2
	% Removal	59%	53%	56%
	Backwash	41 ± 6.5	19 ± 1.8	11 ± 2.1
pCOD	Influent	1019 ± 75.1	920 ± 57.0	1029 ± 31.7
	Effluent	66 ± 40.5	92 ± 30.0	56 ± 10.0
	%Removal	94%	90%	95%
	Backwash	1015 ± 75.4	825 ± 10.7	963 ± 18.4

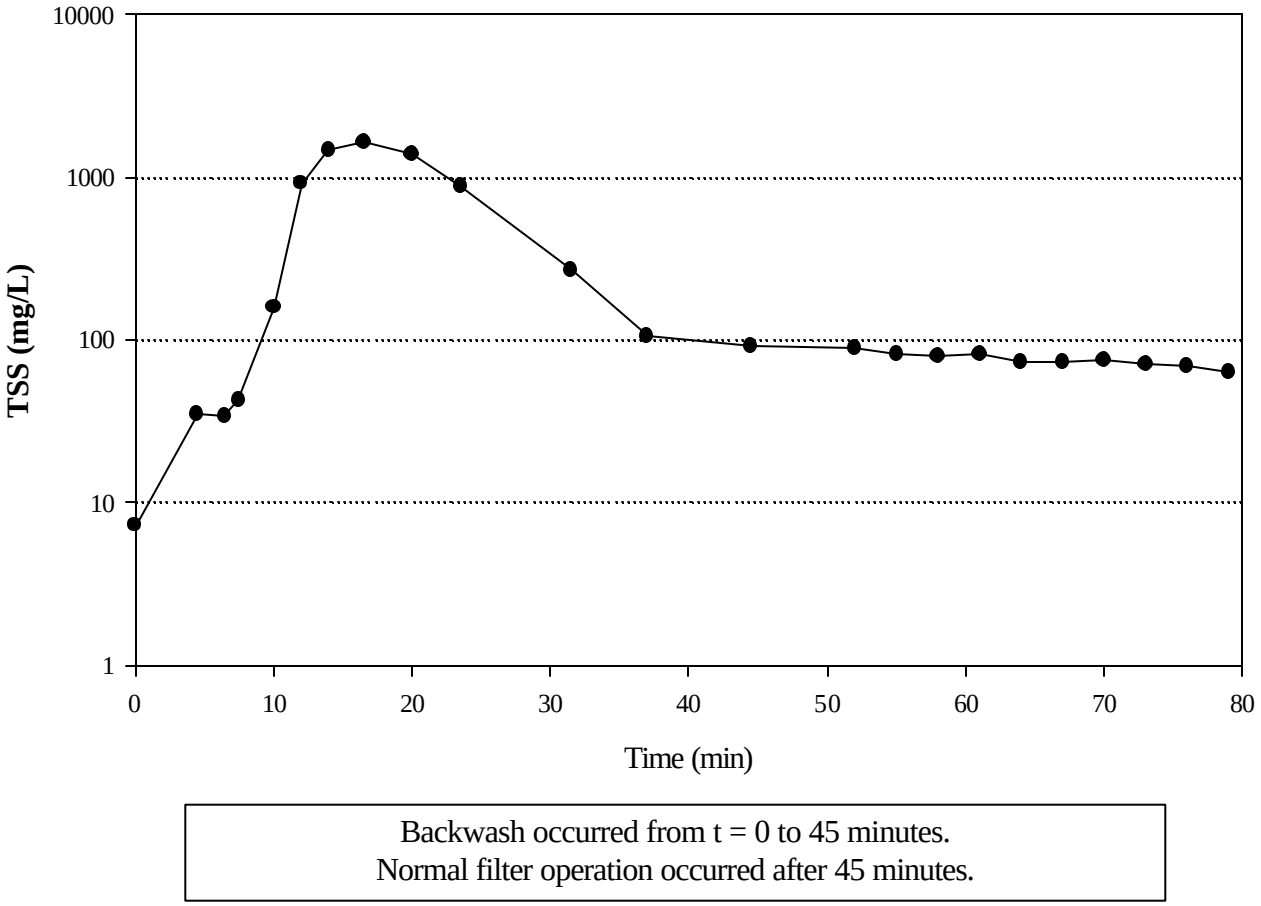

Figure 5: Typical TSS Concentration During and Following a Backwash Sequence on the Full-Scale System

However, the solids removal measured and reported in Table 3 is believed to be lower than what actually occurred. Effluent from the filter bed contains solid material that was applied, which managed to maneuver through the entire bed depth. Additional solids caused by biomass detachment from the media is believed to be present in the effluent. Biomass detachment is caused by a variety of factors, such as fluid shear and weakly attached biomass release from the media. Biomass detachment from the media was believed to occur; however, effluent sample analysis could not distinguish biomass that grew in the biofilter from applied influent particles. Additionally, loose biomass ended up in the effluent sample collected immediately following a filter backwash, as shown in Figure 5. It is believed that loosely attached and/or residual biomass trapped within the media pores was released when the backwash cycle was completed.

Residual biomass would maneuver through the filter bed and was found in the effluent for a significant time after the filter was brought back on-line following a backwash (see Figure 5). During the mass balance investigation, effluent sampling was resumed immediately following the filter bed's backwashing regime. Therefore, effluent samples would collect residual biomass, which remained in the media pores, following backwashing. This would increase the solid material collected in the effluent composite sample, which consequently reduced the solid removal percentage of the filter. The removal of solid material by the BIOFOR® was exceptional, and the actual solids removal was believed to be higher than the measured values indicate.

During the mass balance experiments, the total COD removal ranged from 72 to 77%, whereas the soluble COD removal averaged between 53 to 56% (see Table 3). The measured consumption of soluble material is lower than expected. The lower removal percentage could be due to capture of soluble COD in the effluent composite sampler immediately after the backwash. Cell lysis, production of EPS, and biomass detachment could increase the soluble COD in effluent samples. Additionally, the bulk-liquid accumulation of hydrolyzed particles is another source of soluble COD production within the filter. Differentiation between applied wastewater soluble COD and biomass generated soluble COD was not investigated in this study. Future research is required to determine the net soluble COD flux in the BAF system before conclusions can be made. In contrast, particulate COD removal averaged between 90-95% (see Table 3). The high removal of particulate COD was in agreement with the high solids removal measured for TSS and VSS. The high solids retention in the bed emphasizes why particle hydrolysis is important.

Filter backwash samples were collected to determine the amount of biomass generated during the filter run cycle. Biomass generated during the filter run cycle was assumed to be completely removed by the backwash sequence. Filter backwashing combines several stages of high velocity water and air scours, which expands the filter media. Backwashing provides sufficient shearing velocity by supplying approximately 6 times the velocity during normal filter operation and removes biomass and enmeshed particles. Therefore, the backwash composite sample contains all the newly generated biomass and unhydrolyzed particles applied in the influent

wastewater. Biomass and unhydrolyzed particles removed during the backwashes varied between 700 and 820 kg with the particle COD ranging from 825 to 1015 kg, as shown in Table 3. However, biomass and unhydrolyzed particles could not be readily distinguished from one another in backwash composite samples via a TSS/VSS analysis. Applied particles become enmeshed and lodged inside the attached biomass and were removed during the backwash. If an estimate of the fraction of particles that undergo hydrolysis can be made, then it will be possible to differentiate between applied particles and biomass in backwash composite samples. Hydrolyzed influent particles are consumed by the microorganism as available substrate, which generates additional biomass. Therefore, determining the fraction of particle hydrolysis will also allow the observed biomass yield to be estimated.

Bench-Scale BAF Hydrolysis Experiments

Two hydrolysis experiments were performed at different mass loadings using a bench-scale reactor. The endogenous respiration ΔDO profiles for both experiments are shown in Figures 6 and 7. The ΔDO profiles differ between experiments, but the overall trend was similar. The growth phase duration varied between the two experiments because influent wastewater feeds were collected at different times. The two experiments used different influent wastewater feeds because the experiments were performed at different times, approximately 3 weeks apart. dditionally, the reactor was operated for two days prior to the beginning of the growth phase for the first experiment. The second experiment had limited wastewater feed volume; therefore, no pre-experiment biomass growth phase was performed. The different influent feed characteristics and the pre-experiment growth could be responsible for the different dissolved oxygen (ΔDO) profiles seen for the growth phases shown in Figures 6 and 7.

Initially, oxygen consumption during the endogenous respiration phase increased for approximately 4 hours and was followed by a decay in the measured ΔDO. Both experiments showed a "flat-line" for ΔDO after approximately 10 hours, but a subsequent increase in ΔDO followed in both experiments. Nitrate and nitrite concentrations were analyzed during this same phase for the second experiment and results indicate that the increase in ΔDO was not due to nitrification (data not shown). Therefore, it is unclear why the slight increase in ΔDO occurred. The initial 4 hours of the endogenous respiration phase was not included when determining the

percent hydrolysis due to results collected during the hydrolysis phase, which is discussed later. Data collected during the remaining 20 hours were used to determine the average endogenous ΔDO consumption and total and soluble COD in the reactor's effluent. The ΔDO profiles shown in Figures 6 and 7 were integrated, and the average endogenous ΔDO was calculated to be 3.21 mg/L per HRT for the first experiment and 0.18 mg/L per HRT for the second experiment. Clearly, these average endogenous ΔDO values are different and probably reflect variability between the biomass for each experiment, which was higher in the first experiment. The COD and soluble COD profiles for each experiment are shown in Figures 8 and 9. The mineral salt solution was a carbon free source of influent feed; therefore, the effluent COD and soluble COD values resulted from cell lysis and biomass detachment. During the first experiment, the COD

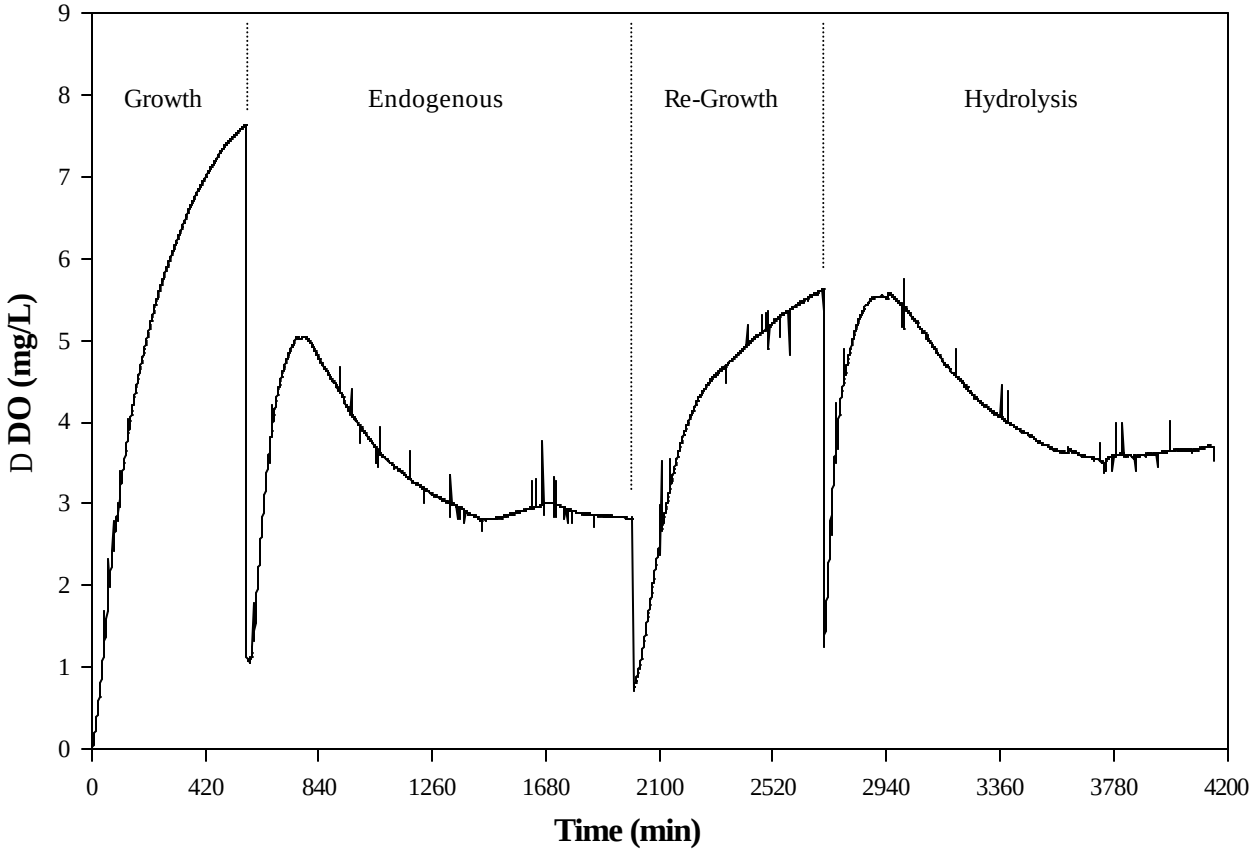

Figure 6: Bench-Scale Reactor ΔDO During the First Hydrolysis Experiment

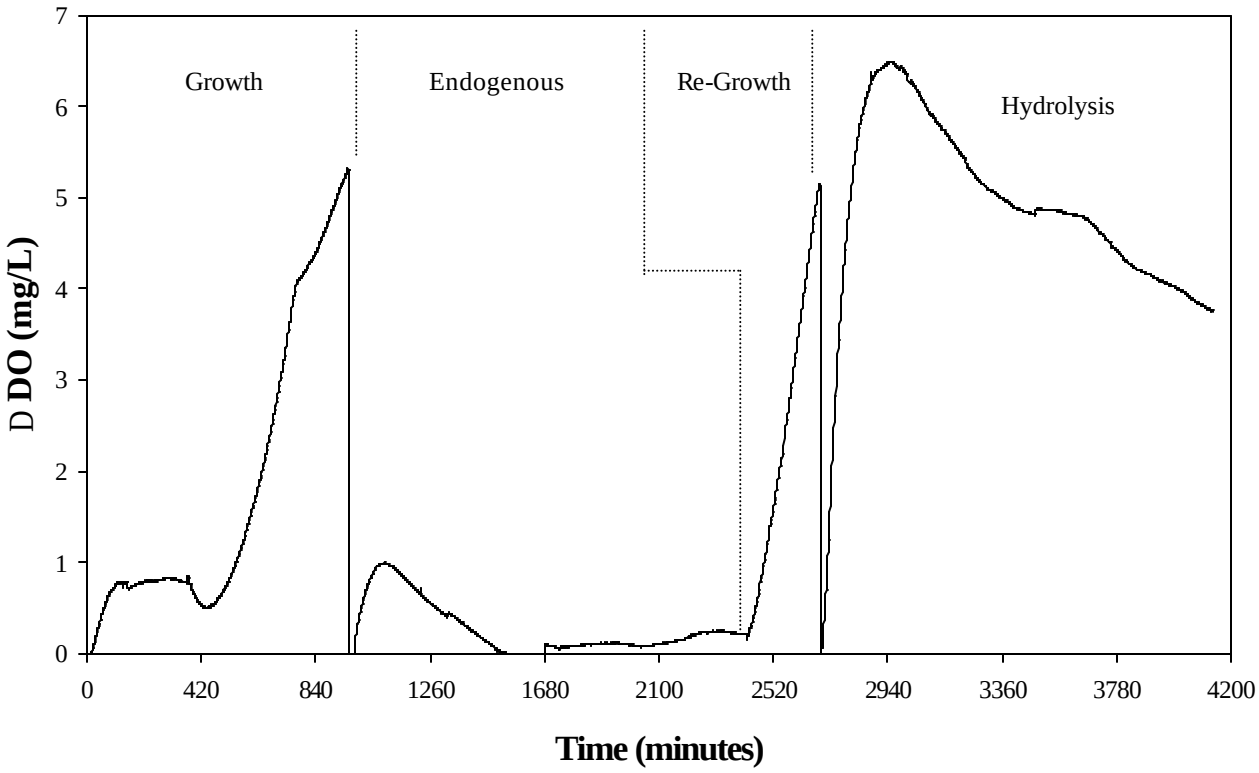

Figure 7: Bench-Scale Reactor ΔDO During the Second Hydrolysis Experiment

and soluble COD profile (see Figure 8) shows significant cell lysis and biomass detachment during the initial 4 hours of the experiment; however, after 9 hours of operation, effluent COD and soluble COD values became negligible. In contrast, cell lysis and biomass detachment was significant throughout the second experiment, as shown in Figure 9, further supporting the variation between the two experiments. The endogenous respiration phase shows the baseline biomass respiration, and COD and soluble COD values caused by cell lysis and biomass detachment for reactor effluent samples from each experiment.

The re-growth phase of the experiment began after the completion of the 24 hour endogenous phase. The re-growth phase re-established biomass growth after 24 hours of "starvation," which allowed endogenous and hydrolysis phase physiological state comparisons to be performed. The first experiment had a re-growth phase lasting approximately 12 hours, and the second experiment re-growth phase operated approximately 6 hours. The duration of the re-growth

phases lasted according to the ability of the biomass to be reactivated following "starvation." Biomass reactivation was monitored by the increase in ΔDO and soluble COD consumption. During re-growth, the first experiment showed a sharp increase DO consumption following reactivation, but a decrease in the rate of DO consumption after approximately 6 hours (see Figure 6). The biomass did not consume DO as readily after 12 hours during the re-growth phase as compared to the growth phase in the first experiment. The difference between the DO consumption could not be identified; however, the biomass was considered reactivated after 12 hours of the re-growth phase because the ΔDO is steadily increasing and indicates a growing biomass. Soluble COD consumed after 12 hours was similar at the completion of both growth and re-growth phases during the first experiment. In contrast, biomass seemed to be reactivated immediately after the re-growth phase was initiated in the second experiment, as shown in Figure 7. Reactivation of the biomass was a critical component, which allowed a physiological comparison of the biomass during endogenous and hydrolysis phases of the experiments.

At the completion of the re-growth phase, soluble COD and ΔDO values were used to calculate two important parameters, as shown in Table 4. First, influent and effluent soluble COD values were measured at the end of the re-growth phase. Soluble COD consumed during one HRT was calculated from the difference between influent and effluent samples at the completion of the re-growth phase. The difference between influent and effluent soluble COD was 12.65 mg/L for the first experiment and 17.53 mg/L for the second experiment. Therefore, the mass of soluble COD consumed during one HRT could be calculated, and the values were 2.30 mg for the first experiment and 3.19 mg for the second experiment. Additionally, the ΔDO at the completion of each re-growth phase was determined, with the first experiment having 5.62 mg/L DO consumed and the second experiment having 4.84 mg/L consumed during one HRT. A ratio of mg soluble COD per ΔDO was calculated. As shown in Table 4, the ratios of 0.41 and 0.66 mg soluble COD per ΔDO were calculated for the first and second experiment, respectively. The soluble COD/ΔDO ratio gives the oxygen required to consume soluble COD during one HRT. The soluble COD/ΔDO ratio is an important parameter because it normalizes each experiment to a common parameter, in this case ΔDO. For every ΔDO reading during the hydrolysis phase, the soluble COD consumed is known. The soluble COD/ΔDO ratio was used to determine the

amount of soluble COD consumed during the hydrolysis phase. A key assumption is that solubilized material that came from the hydrolyzed particles were identical to the soluble COD consumed during the re-growth phase.

Table 4: Bench-Scale Reactor Data and Hydrolysis Calculation

		Experiment #1	Experiment #2
1	HRT	65 minutes	65 minutes
2	Flowrate	2.8 mL/min	2.8 mL/min
3	Average ΔDO during Hydrolysis Phase	4.020 mg/L per HRT	4.869 mg/L per HRT
4	Average ΔDO during Endogenous Phase	3.213 mg/L per HRT	0.180 mg/L per HRT
5	ΔDO Difference	0.807 mg/L per HRT	4.689 mg/L per HRT
6	Applied sCOD during Re-growth Phase	77.02 mg/L	73.97 mg/L
7	Effluent sCOD during Re-growth Phase	64.37 mg/L	56.44 mg/L
8	sCOD Difference	12.65 mg/L	17.53 mg/L
9	Mass of sCOD consumed in one HRT (Row 8 *x* Row 1 *x* Row 2)	2.30 mg	3.19 mg
10	ΔDO consumed over one HRT during Re-growth Phase	5.62 mg/L	4.84 mg/L
11	Ratio of sCOD / ΔDO (Row 9 / Row 10)	0.410 mg sCOD/ΔDO	0.659 mg sCOD/ΔDO
12	Time during Hydrolysis Phase (after initial 4 hours of washout)	1200 min	1200 min
13	Total number of HRTs (Row 12 / Row 1)	18.5 HRTs	18.5 HRT
14	ΔDO consumed due to Solubilized Particles (Row 5 x Row 13)	14.9 mg/L	86.8 mg/L

The hydrolysis phase of the experiment lasted 24 hours, the same as the endogenous respiration phase. Particles were introduced into the column as a spike input. The spike input was used because of possible clogging of the filter if continuous particle feed was implemented. The initial 4 hours of the hydrolysis phase was used as a washout period similar to Larsen and Harremoës (1997). In Larsen and Harremoës's experiment, they included a 15 minute (or 13 HRTs) washout stage to remove unattached and loosely attached particles that were applied. The experimental design in this investigation had a much longer reactor HRT and slower flow rates than Larsen and Harremoës's experimental design. The bench-scale reactor in this experiment was designed to match the full-scale BAF system and was modeled on the full-scale empty bed volume. Therefore, it was assumed no additional applied particulate material washed out of the system when effluent endogenous respiration phase COD values exceeded effluent hydrolysis phase COD values (experiment 1) or when effluent soluble COD equaled the effluent COD during the hydrolysis phase (experiment 2) as shown in Figures 8 and 9, respectively. With this assumption, applied particles stopped washing out of the reactor after 4 hours of operation during both experiments. Additionally, the applied particle solution had soluble COD associated with it. The soluble COD in the particle solution was a consequence of soluble materials (<1.5 µm) detaching from larger particles, and the initial ΔDO increase reflects this. Both experiments show a ΔDO peak approximately at the fourth hour into the hydrolysis phase, this further supports the elimination of the first 4 hours of the hydrolysis phase and suggests that soluble substrate was no longer detaching from the applied particles. In other words, the main substrate source prior to 4 hours was detaching soluble COD and not hydrolyzed particles. In summary, in this investigation particle hydrolysis was assumed to occur after the initial 4 hours of the hydrolysis phase for both experiments.

The initial particle mass applied to the reactor varied between experiments. Particle COD concentrations were varied to determine if the mass of particles applied had an effect on particle hydrolysis. During the first experiment, the particle COD applied was 189 mg/L, and the second experiment applied 1,160 mg/L particle COD. After the washout of particles concluded, the initial mass of particles in the reactor during the first experiment was 15.3 mg particle COD and the second experiment had 123.3 mg particle COD. The initial mass of particles at the start of hydrolysis measurements had to be known before the percent hydrolysis could be calculated.

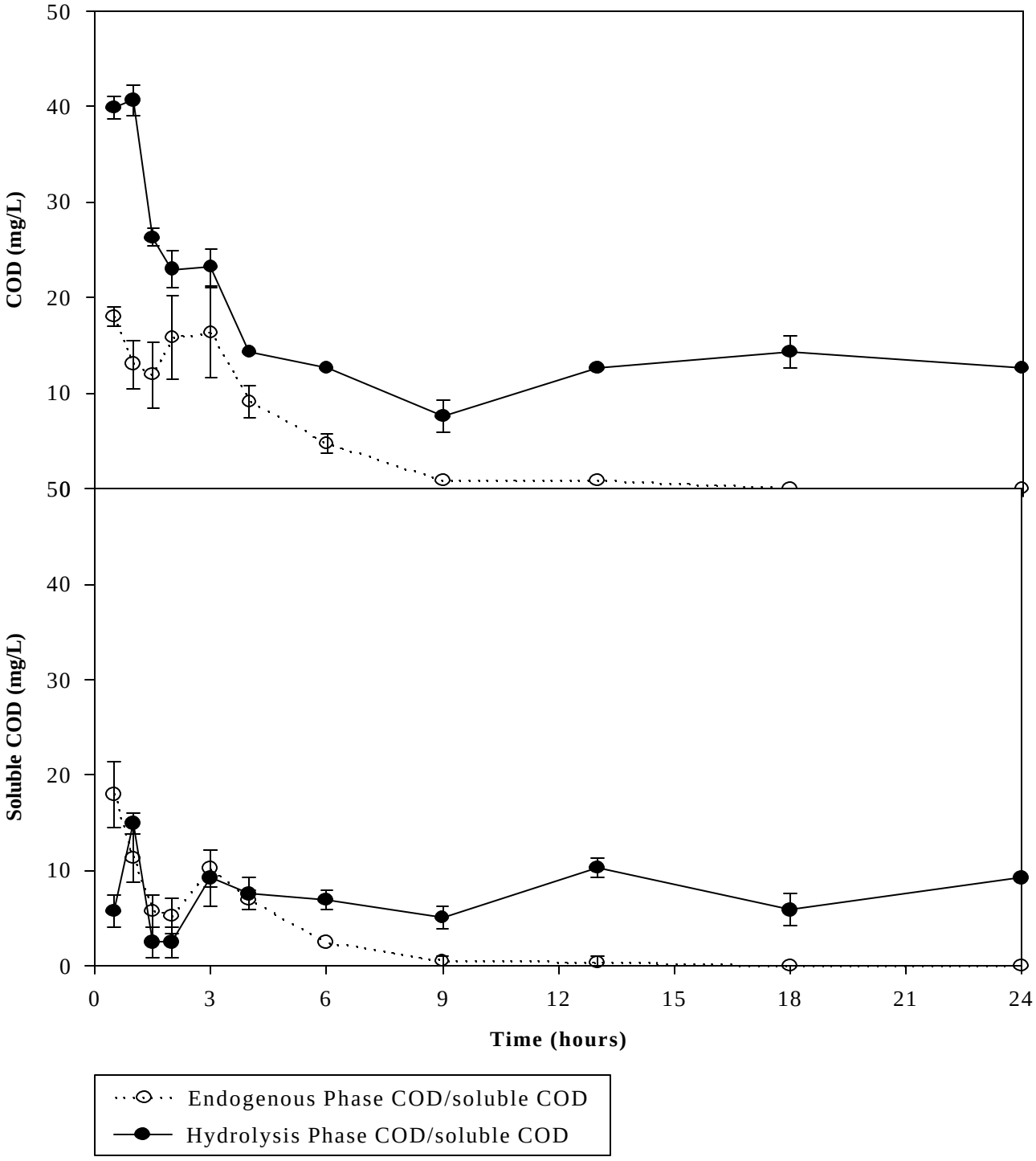

Figure 8: COD and Soluble COD Profiles for the First Hydrolysis Experiment

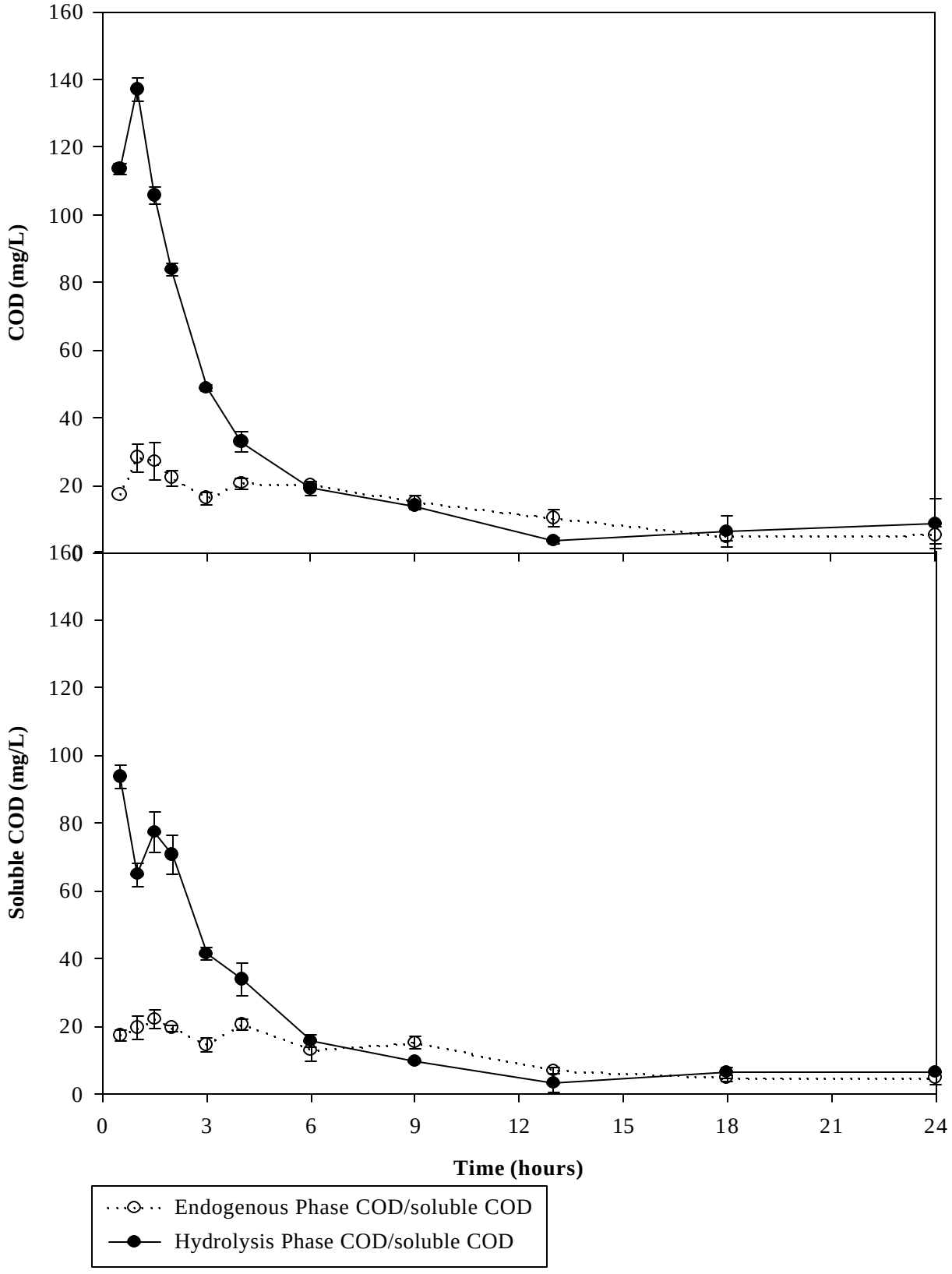

Figure 9: COD and Soluble COD profiles for the Second Hydrolysis Experiment

After the initial 4 hours, the average ΔDO measured during the hydrolysis phase of the first experiment was 4.02 mg/L and 4.87 mg/L during the second experiment. The endogenous respiration ΔDO concentration was subtracted from the hydrolysis phase ΔDO concentration giving the hydrolytic ΔDO concentrations of 0.81 mg/L for the first experiment and 4.69 mg/L for the second experiment as shown in Table 4. These values indicate the consumption of solubilized COD, which was available only due to the hydrolysis of applied particulate matter. The ΔDO measurement indicates the COD equivalent mass of hydrolyzed particles by using the soluble COD/ΔDO ratio calculated during the re-growth phase. During the first experiment, 6.1 mg of applied particles were consumed as solubilized COD, which equates to a 40.0% hydrolysis efficiency. During the second experiment, 57.1 mg of applied particles as COD were hydrolyzed and consumed, giving a hydrolysis value of 46.3%.

Despite many variations between the experiments, such as influent feed and mass of particles applied, hydrolysis values were very similar. A key assumption is that solubilized material that came from the hydrolyzed particles were identical to the soluble COD consumed during the re-growth phase. The particulate material was taken from the same full-scale BAF influent sample as the applied soluble COD used during the re-growth phase. An additional assumption was that hydrolyzed particles were immediately consumed once hydrolyzed, and solubilized material from particles did not wash out of the system. Therefore, if a particle was hydrolyzed into a monomer, it was consumed as soluble COD by the biomass. A final assumption was that the physiological states of the biomass were similar at the beginning of the endogenous respiration phase and hydrolysis phases. This assumption is believed to be true due to inclusion of the re-growth phase in between the two phases, i.e. the growth phase prior to the endogenous and hydrolysis phase was the same. With these assumptions, the hydrolysis percentages were calculated and were applied to the full-scale mass balance to determine the biomass yield for the BAF treatment system.

Full-Scale Biomass Yield Calculations

Full-scale biomass yield calculations were performed after determining the hydrolysis of particulate material. The full-scale BAF system retained a high percentage of applied particulate matter, as shown in Table 2. The retained particulate matter contained a large amount of

substrate, which required hydrolysis before being utilized by the biomass as substrate. The mass of energy available in the retained particulate matter (> 1.5 µm) ranged from 827 to 973 kg of COD (Row 1), as shown in Table 5. Assuming an average hydrolysis of 43%, hydrolyzed particle masses ranged from 356 to 418 kg of COD (Row 3) after using the hydrolysis values calculated from the bench-scale reactor. Clearly, particle hydrolysis is a significant source of substrate and energy available to the biomass and oxygen demand to be satisfied by the blowers, in the BAF system. The hydrolyzed particles are consumed and therefore converted into new biomass cells or are used for maintenance and growth of the existing biomass. The backwash composite sample was differentiated into two fractions, the residual unhydrolyzed particles and new biomass removed during the backwash. The backwash composite sample ranged from 844 to 1056 kg COD (Row 5), and the residual un-hydrolyzed particulate matter varied from 471 to 555 kg COD (Row 4) as shown in Table 5. The difference between the two values is the mass of biomass (as COD) removed during the backwash sequence. New biomass COD values varied between 373 and 512 kg COD (Row 6), as shown in Table 5.

Table 5: Biomass Yield Calculation for Full-Scale BAF Using an Average Percent Hydrolysis of 43%

		Experiment #1	Experiment #2	Experiment #3
1	Mass of pCOD Retained in Filter	954	827	973
2	% Hydrolysis	43%	43%	43%
3	Mass of pCOD Solubilized and Consumed by Biomass	410	356	418
4	Mass of Un-hydrolyzed pCOD Residual Left in Filter	544	471	555
5	Total Mass of COD Collected during Backwash	1056	844	974
6	Generated Biomass COD (Row 5 – Row 4)	512	373	419
7	Soluble Substrate Consumed (from Table 3: the difference between applied soluble COD and effluent soluble COD concentrations)	688	482	492
8	Total Consumed Substrate as COD (Row 3 + Row 7)	1098	838	910
9	**Yield (Row 6/Row 8)**	**0.47**	**0.45**	**0.46**

The mass of substrate consumed is the final parameter for the determination of biomass yield. The addition of soluble COD consumed (see Table 5) and the available COD from solubilized particles equals the total mass of substrate consumed. The applied soluble substrate consumed varied between 482 and 688 kg COD (Row 7), and the mass available due to particle hydrolysis ranged from 356 to 418 kg of COD (Row 3), as shown in Tables 5. Therefore, total substrate consumption was between 838 and 1098 kg COD. The observed yield calculations were performed using the mass of biomass removed during backwash and the total mass of substrate consumed. The observed yield coefficient for the full-scale BAF system varied between 0.45 and 0.47 mg biomass COD/mg substrate consumed as COD as shown in Table 5.

Cell-Free Extracellular Enzyme Quantification

Currently, two hypotheses have been proposed to describe the mechanistic degradation and hydrolysis of particles. Both hydrolysis hypotheses require MBEE to hydrolyze particles attached to the biofilm. Larsen and Harremoës (1994) suggest CFEE hydrolyze large particles in the bulk-liquid as an initial step. Confer and Logan (1997a) propose bulk-liquid hydrolysis is negligible in particle hydrolysis. Investigations were performed during this study to determine if bulk-liquid hydrolysis of particulate matter was detectable. Larsen and Harremoës developed a simple model to measure the bulk-liquid hydrolysis of particles by CFEE. The model was used to compare the measured values in this investigation to the theoretical model proposed.

Larsen and Harremoës (1994) formulated the following equations for the determination of bulk liquid hydrolysis by CFEE. Bulk liquid hydrolysis (R, (mass/volume-time)) is formulated from the second order bulk liquid hydrolysis constant (k, (volume/IU-time, where IU:international unit)), non-diffusible substrate (X_s, mass COD/volume) concentration, and free extracellular enzyme concentration (S_e, IU). The equations are:

Bulk liquid hydrolysis $R = k X_s S_e$

Where $$k = \frac{Q^2}{A V p_e \left(\frac{1}{D_h} - 1 \right)}$$ (Equation 1)

The variable p_e is the biofilm production rate of extracellular enzymes.

$$p_e = \frac{S_e Q}{A}$$

Where:

D_h = hydrolysis coefficient (mass/mass)

A = biofilm surface area (length^2)

V = bulk liquid volume (length^3)

Q = volumetric flow rate (volume/time)

An interesting point must be made about the CFEE model. First, if the second order bulk liquid hydrolysis constant (k) and the biofilm production rate of extracellular enzymes (p_e) are substituted into the bulk liquid hydrolysis equation, the free extracellular enzyme concentration (S_e) is eliminated from analysis.

$$R = \frac{X_s}{T_{HRT}\left(\frac{1}{D_h} - 1\right)} \qquad \text{(Equation 2)}$$

Where T_{HRT} is the hydraulic residence time in the bench-scale reactor.

Therefore, the model proposed by Larsen does not solely consider bulk-liquid hydrolysis, but total hydrolysis from both CFEE and MBEE. The model does not differentiate between the two mechanistic hydrolytic functions. Therefore, the model does not measure the hydrolysis of particles in the bulk liquid only; rather, the model measures hydrolysis by both CFEE and MBEE.

During the second experiment, CFEE activity was monitored using FDA as the model substrate. CFEE hydrolytic activities were measured for both the endogenous and hydrolysis phases. The bulk liquid hydrolysis by CFEE increased in the hydrolysis phase relative to the endogenous phase, as shown in Figure 10. Quantification of bulk liquid hydrolysis was not possible due to the complexity of the hydrolysis mechanism. In conclusion, bulk liquid hydrolysis increased

during the hydrolysis phase in comparison to the endogenous phase, but the importance of bulk liquid hydrolysis and CFEE could not be quantified. Further research is required before the role of bulk-liquid hydrolysis by CFEE is known.

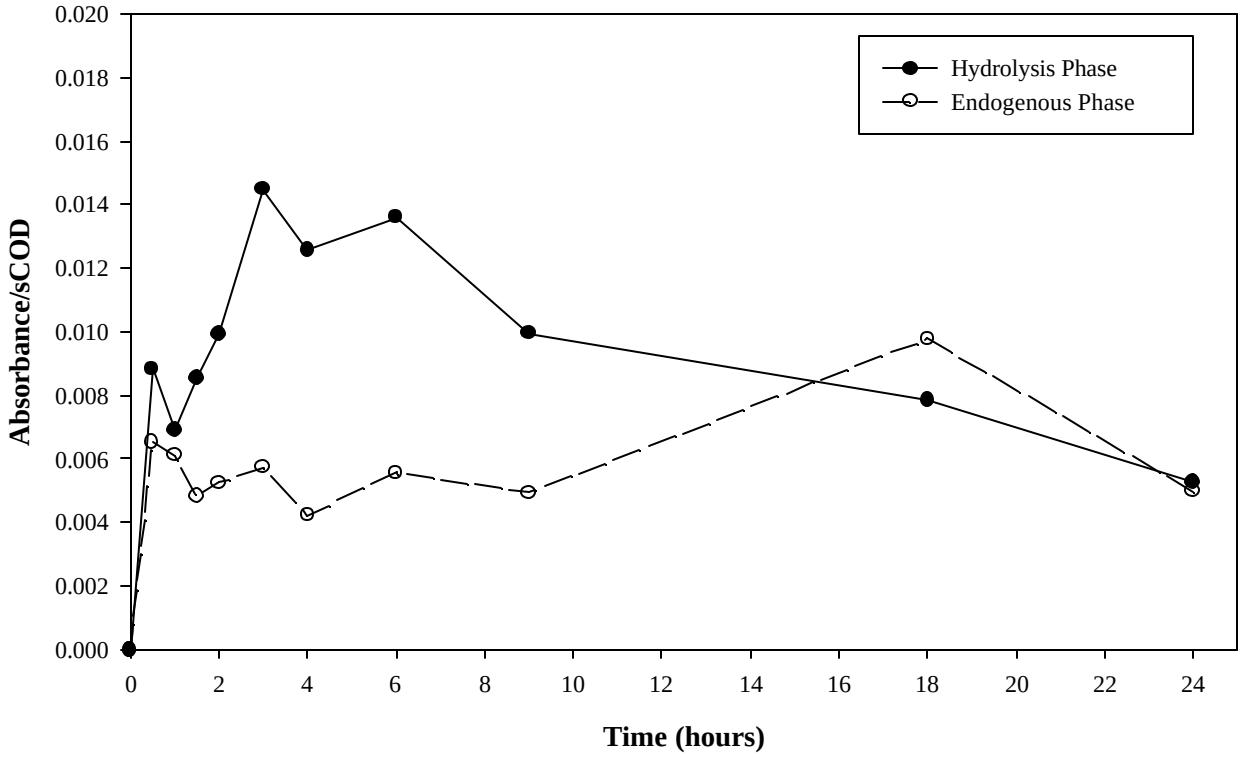

Figure 10: Bulk-Liquid Hydrolysis Estimation using FDA

Conclusions

Observed biomass yield and particle hydrolysis quantification was performed for a full-scale BIOFOR® biological aerated filter. Mass balances were performed on the full-scale system to quantify the consumption of soluble COD and the particulate material filtered from the waste stream. The particulate material required hydrolytic enzymes to convert the large polymers into smaller monomers before becoming available as a viable source of energy for the biomass. A bench-scale reactor was designed and constructed to quantify the degree of hydrolysis of applied particulate matter. Two bench-scale experiments were performed to characterize the degree of hydrolysis of applied BAF influent wastewater particulate matter. The percentage of applied particles hydrolyzed was found to be 40% and 46.3% from two bench-scale experiments, and subsequently consumed by the biomass. The biomass observed yield was found to range

between 0.43 to 0.48 mg biomass COD generated per mg substrate COD consumed. The mechanistic degradation of particulate matter was also investigated to determine whether CFEE were a contributor to the overall hydrolysis process. Bulk-liquid hydrolysis increased during the hydrolysis phase relative to the endogenous phase, which suggests CFEE may contribute to particle solubilization. However, bulk-liquid hydrolysis and CFEE roles in the degradation of particulate matter could not be quantified.

Particle hydrolysis and biomass yield estimations are important parameters when designing aeration systems and solids handling facilities at wastewater treatment facilities. Particle hydrolysis constituents 42 $\pm$ 4.3% of the oxygen demand for the full-scale BAF treatment system. Therefore, knowledge of hydrolysis leads to a better understanding of how to evaluate aeration blower design for full-scale BAF system. Additionally, the solubilization of particulate matter reduces the mass of solids handling between 400 to 500 lbs/day, which impacts the design of solids handling facilities. Finally, biomass yield estimations aid wastewater treatment facilities in estimating the rate of biomass wastage from biological treatment processes.

References:

Aesoy, A. and Odegaard, H. (1994) Denitrification in biofilms with biologically hydrolyzed sludge as a carbon source. Water Science & Technology, 29 (10/11), 93-100.

Amar, D., et al. (1986) The use of an up-flow fixed bed reactor for treatment of a primary settled domestic sewage. Water Research. 20, 9-14.

American Public Health Association; American Waterworks Association; and Water Environment Federation. (1995) *Standard Methods for the Examination of Water and Wastewater*. 19th Ed., Washington, D.C.

Antizar-Ladislao, B., Katz, S., and Galil, N. (2000) Phenol remediation by biofilm developed in sand soil media. Water Science & Technology, 42 (1/2), 99-106.

Arcangeli, J. and Arvin, E. (1994) Kinetics of toluene degradation in a biofilm system under denitrifying conditions. Water Science & Technology, 29 (10/11) 393-400.

Arcangeli, J. and Arvin, E. (1997) Modelling of the growth of a methanotrophic biofilm. Water Science & Technology, 36 (1), 199-204

Barlindhaug, J. and Odegaard, H. (1996) Thermal hydrolysate as a carbon source for denitrification. Water Science & Technology, 33 (12), 99-108

Boczar, B., Begley, W., and Larson, R. (1992) Characterization of enzyme activity in activated sludge using rapid analyses for specific hydrolases. Water Environment Research, 64, 792-797.

Bouwer, E. (1987) Theoretical investigation of particle deposition in biofilm systems. Water Research, 21, 1489-1498

Carrand, Capon, Rascont, Brenner. (1990). Elimination of carbonaceous and nitrogenous pollutants by a twin-stage fixed growth process. Water Science & Technology, 22 (1-2), 261-272.

Characklis, W. and Marshall, K. (1990) Biofilms. Wiley Interscience, John Wiley and Sons. Toronto, Canada.

Chróst, R. (1989) Characterization and significance of ß-glucosidase activity in lake water. Limnology and Oceanography 34, 660-672.

Confer, D. and Logan, B. (1991) Increased bacterial uptake of macromolecular substrates with fluid shear. Applied Environmental Microbiology, 57, 3093-3100.

Confer, D. and Logan, B. (1997a) Molecular weight distribution of hydrolysis products during biodegradation of model macromolecules in suspended and biofilm cultures I. Bovine serum albumin. Water Research, 31 (9), 2127-2136.

Confer, D. and Logan, B. (1997b) Molecular weight distribution of hydrolysis products during biodegradation of model macromolecules in suspended and biofilm cultures II. Dextran and destrin. Water Research, 31 (9), 2137-2145.

Confer, D., Logan, B., Aiken, B., and Kirchman, D. (1995) Measurement of dissolved free and combined amino acids in unconcentrated wastewaters using high performance liquid chromatography. Water Environment Research, 67, 118-125.

de Beer, D., Stoodley, P., Roe, F., Lewandowski, Z. (1993) Effects of biofilm structure on oxygen distribution and mass transport. Biotechnology and Bioengineering, 43, 1131-1138.

De Rosa, S., Sconze, F., and Volterra, L. (1998) Biofilm amount estimation by fluorescein diacetate. Water Research, 32(9), 2621-2626.

Fleming, H. (1995) Sorption sites in biofilms. Water Science & Technology, 32 (8), 27-33.

Fontvieille, D., Outaguerouine, A., and Thevenot, D. (1992) Fluorescein diacetate hydrolysis as a measure of microbial activity in aquatic systems: Application to activated sludges. Environmental Technology, 13, 531-540.

Green, M., Ruskol, Y., Lahav, O., and Tarre, S. (2001) Chalk as the carrier for nitrifying biofilm in a fluidized bed reactor. Water Research, 35 (1), 284-290.

Haldane, G. and Logan, B. (1994) Molecular size distributions of a macromolecular plysaccharide (dextran) during its biodegradation in batch and continuous cultures. Water Research, 28 (9), 1873-1878.

Hollibaugh, J. and Azam, F. (1983) Microbial degradation of dissolved proteins in seawater. Limnology and Oceanography, 28, 1104-1116.

Hoppe, H. (1983) Significance of exoenzymatic activities in the ecology of brackish water: measurements by means of methylumbelliferyl-substrates. Marine Ecology Progress Service, 11, 299-308.

Horan, N. and Eccles C. (1986) Purification and characterization of extracellular polysaccharide from activated sludges. Water Research, 20, 1427-1432.

Karamanev, D. and Samson, R. (1998) High-rate biodegradation of pentachlorophenol by biofilm developed in the immobilized soil bioreactor. Environmental Science & Technology, 32 (7), 994-999.

Koch, G. and Siegrist, H. (1997) Denitrification with methanol in tertiary filtration. Water Research, 31 (12) 3029-3038

Larsen, T., and Harremoës, P. (1994) Degradation mechanisms of colloidal organic matter in biofilm reactors. Water Research, 28, 1443-1452.

Law, B. (1980) Transport and utilization of proteins by bacteria. In *Microorganisms and Nitrogen Sources*. Edited by Payne, J. Wiley, New York, NY. 381-409.

Lazarova, V. and Manem, J. (1995) Biofilm characterization and activity analysis in water and wastewater treatment. Water Research, 29 (10), 2227-2245.

Levine, A., Tchobanoglous, G., and Asano, T. (1985) Characterization of the size distribution of contaminants in wastewater: treatment and reuse implications. Journal of Water Pollution Control Federation, 57, 805-816.

Lewandowski, Z., Stoodley, P., Altobelli, S., and Fukushima, E. (1994). Hydrodynamics and kinetics in biofilm systems: Recent advances and new problems. Water Science & Technology, 29, 223-229.

Logan, B., Hermanowicz, S., and Parker, D. (1987a) Engineering implications of a new trickling filter model. Journal of Water Pollution Control Federation, 59, 1017-1028.

Logan, B., Hermanowicz, S., and Parker, D. (1987b) A fundamental model for trickling filter process design. Journal of Water Pollution Control Federation, 59, 1029-1042.

McLoughlin, A. and Crombie-Quality, M. (1983) The kinetics of protein removal by activated sludge. Water Research, 17, 161-166.

Metcalf and Eddy, Inc. (1991) *Wastewater Engineering: Treatment, Disposal, Reuse.* McGraw-Hill, New York.

Ong, S., et al. (2000) Nitrate removal by an ultra-compact biofilm reactor. Water Science & Technology, 42 (3/4), 137-142.

Pavlostathis, S. and Giraldogomez, E. (1991) Kinetics of anaerobic treatment. Water Science & Technology, 24 (8), 35-59

Pavoni, J., Tenney, M., and Echelberger, W. (1972) Bacterial exocellular polymers and biologicical flocculation. Journal of Water Pollution Control Federation, 44, 414-431.

Pujol, Hamon, Kandel, and Lemmel. (1994). Biofilters: flexible, reliable biological reactors. Water Science & Technology, 29 (10-11), 33-38.

Pujol. (2000). Process improvements for upflow submerged biofilters. Water, 21 (4), 25-29.

Richard, Y. and Seyfield, C. (1987) Advantages of dual media dry filters in biological wastewater treatment. Water Science & Technology, 19 (5/6), 993-1002.

Sagberg, P., Dauthuille, P., and Hamon, M. (1992) Biofilm reactors: a compact solution for the upgrading of wastewater treatment plants. Water Science & Technology, 26 (3/4), 733-742.

Schnurer, J. and Rosswall, T. (1982) Fluorescein diacetate hydrolysis as a measure of total microbial activity in soil and litter. Applied Environmental Microbiology, 43, 1256-1261.

Siegrist, H. and Gujer, W. (1985) Mass transfer mechanisms in a heterotrophic biofilm. Water Research, 19, 1369-1378.

Somville, M. and Billen, G. (1983) A method for determining exoproteolytic activity in natural waters. Limnology and Oceanography, 28, 190-193.

Song, K. and Young, J. (1986) Media design factors for fixed-bed filters. Journal of the Water Pollution Control Federation. 58 (2), 115–121.

Stoodley, P., de Beer, D., and Lewandowski, Z. (1994) Liquid flow in biofilm systems. Applied Environmental Microbiology, 60, 2711-2716.

Swisher, R. and Carroll, G. (1980) Fluorescein diacetate hydrolysis as an estimator of microbial biomass on coniferous needle surfaces. Microbial Ecology, 6, 217-226.

Tago, Y. and Aida, K. (1977) Exocellular mucopolysaccharide closely related to bacterial floc formation. Applied Environmental Microbiology, 34, 308-314.

Zhang, T. and Bishop, P. (1994) Density, porosity and pore structure of biofilms. Water Research, 28, 2267-2277.